



E-ISSN: 2707-8272
P-ISSN: 2707-8264
IJRCET 2021; 2(1): 21-24
Received: 14-01-2021
Accepted: 18-03-2021

Ganiyu Oshinowo
Bowen University
Iwo, Osun State
Nigeria

Evaluation of ocean modeling in presence of radiation

Ganiyu Oshinowo

Abstract

Energy efficiency is the key to achieve sustainability in green building. Lowering the energy consumption in construction is starting to become a significant improvement chance for many organizations. This research will identify the benefits of energy efficiency, explore the methods to apply efficient energy usage in green building, and explore the obstacles in attaining energy efficiency in green building. Even though green buildings use a lesser amount of energy compare with usual building, energy efficiency still hard to achieve, due to some barriers to put into practice energy efficiency. This study will interview a property development company in Malaysia. After analysis, energy efficiency contributed two main benefits in the company such as reduced greenhouse gases emission and lower the air pollution problem, and energy saving. The company implemented electrical feeding and sensor system in lighting system, passive design, and cross ventilation to achieve energy efficiency in their development projects. However, cost barrier, information barrier, and outdoor condition and climate barrier are the obstacles in attaining energy efficiency practices. Due to the time constrain, this research only able to interview one company. With the aim of getting more accurate result, should be interview more companies in the future research because of the energy efficiency cover a wide area in the construction field.

Keywords: mesoscale eddies; relative wind; current-wind

Introduction

The roiling individual of forcefulness between standard pressure and large indefinite quantity is typi-cally declared as a surface wind tenseness, as measured via a bulk statement parameterisation. This relates the wind stress to the variation between the atmospheric wind, commonly at an peak of 10 m, and the surface ocean velocity: $5\tau_s = \rho_a c_d |U_{10} - u_s| (U_{10} - u_s)$, (1) where τ_s is the skin-deep wind stress, ρ_a is the atmospheric density, c_d is the drag coefficient, U_{10} is the 10 m atmospheric wind and u_s is the surface ocean velocity. Written account that the drag constant may also be a utility of $U_{10} - u_s$. Coastal flooding poses a major threat to coastal communities worldwide² and its adverse impacts are expected to increase over the next period (e.g., 3IPCC, 2014; Hallegatte *et al.*, 2013; Hinkel *et al.*, 2014). An effective response⁴ to imminent coastal flooding requires a model that can accurately predict⁵total liquid level (TWL) with lead times of hours to order ten days. There is also a need for decadal criterion projections of probability distributions of⁷TWL, and thus implosion therapy endangerment, under plausible mood change setting.

One of the demand in developing an accurate model of TWL is that¹¹the foretelling of tide and increase, the dominant components of TWL for many seaward regions, is essentially a global problem. What is more, tides and surges¹³at the coast are also influenced by local chance variable in bathy metry through its event on harbour and shelf-scale resonances, move guides for coastal trapped¹⁵waves, and tide-surge interaction. This wide extent of spatial scales makes¹⁶the choice of the grid placement for the model quibbling.

Corresponding Author:
Ganiyu Oshinowo
Bowen University
Iwo, Osun State
Nigeria

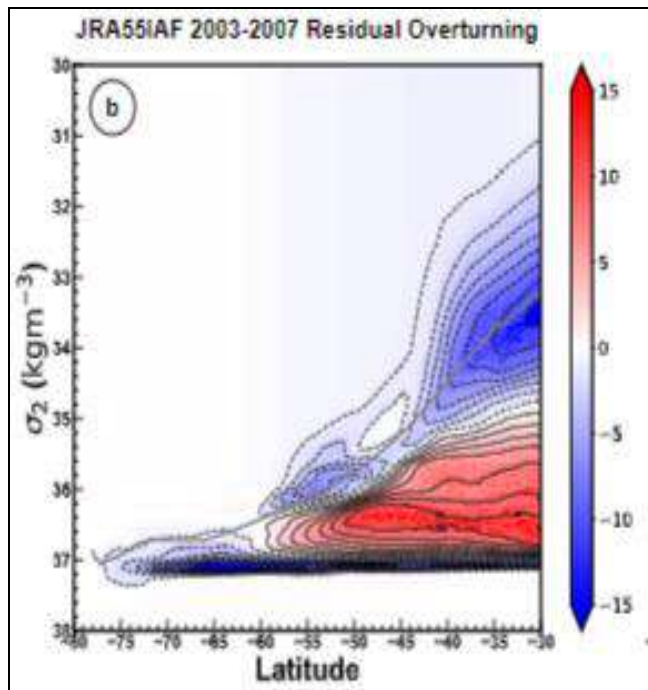


Fig 1: Latitude Analysis

Although improvements in purely hydraulics (also referred to as “forward”) globular tidal models have been made through the increase of self-attraction and loading, and geography internal wave drag (e.g., Kodaira *et al.*, 2016b), further improvements are required to improve the polymerization of sub-grid scale processes. It is well known that the oceanic tide can be excited by the atmospheric tide forced by the thermal effect of radiation, mostly at the solar diurnal (S1) and semidiurnal (S2) frequencies (e.g., Cartwright, 1978). The atmospherically-forced limitless tides will henceforward be referred to as “radiation” tides (Munk and Cartwright, 1966) and written account by $rS1$ and $rS2$. The abundance of $rS1$ is comparatively small (~1 cm) in contrast to the amplitude of $rS2$ which can be 5-10 cm (Cartwright, 1978). Similar to the gravitational tide, $rS2$ is generated primarily over the tropical oceans and has a global response. As a result, $rS2$ will be missed in regional flood forecasting systems if it is not included through the open line conditions. Furthermore, the part power for the ocean models must have sufficiently high temporal resolving power in order to properly resolve $rS2$ (Dobslaw and Thomas, 2005). The main goal of the present study is the development of a computationally efficient scheme for inaccurately predicting the global distribution of TWL. This leads us to two questions of practical and scientific uninterestingness. The first question is how can we best predict period using a model with limited spatial resolution? A simple motion would be to straight off poke at the modelled tides towards tidal observations (e.g., Han *et al.*, 2010; Fu *et al.*, 2021). However, this approach is not suitable for TWL because the surge section of TWL will be suppressed by the poke at. In this study, we use a modified form of spectral nudging (Thompson *et al.*, 2006) to target specific tidal frequency bands there by reducing the suppression of the upsurge. Following Kodaira *et al.* (2019), we refer to this qualified skillfulness as “tidal nudging”.

Ocean Model

The tidal nudging epistemology is further unregenerate in Appendix B. It is shown that tidal nudging of currents in the momentum equation is preferable to adding a sea level nudging term of the form $\lambda (\eta_{obs} - \eta)$ to the precise side of the continuity equation, (2). The governing equations are solved definite quantity using the NEMO modelling framework (Madec, 2008). The hypothesis grid is the extended version of a tri-polar ORCA grid (referred to as eORCA12). It has a nominal resolution of $1/12^\circ$ at the equator. In equivalence with the new version of ORCA12, the eORCA12 grid has been extended due south from $77^\circ S$ to $85^\circ S$ in order to allow tidal propagation under Antarctic ice shelves. Such propagation is necessary for accurate tide predictions throughout the Southern Ocean and potentially the tropics. (De Kleermaeker *et al.*, 2017). Urvey (Remo *et al.*, 2008). The model is 2D barotropic with one single steep layer in the water column.

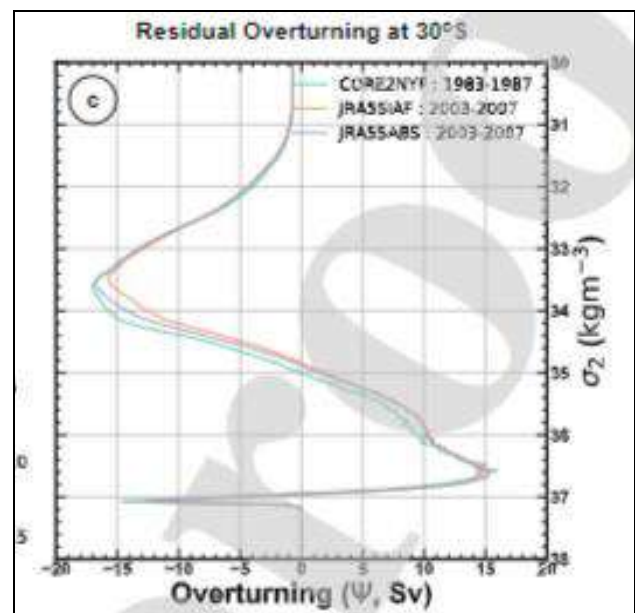


Fig 2: Analysis of Overturning

The hypothesis is run with a baroclinic time period step of 180 s and a mode-cacophonous subroutine is then unemployed to solve the barotropic consider using a time step of 6s. For computational efficiency, all superfluous calls to subroutines related to vertical processes and tracers were removed. Tidal nudging was applied at every baroclinic time period step. The quadratic bottom friction was parameterized using a constant drag coefficient of 2.5×10^{-3} . To history for the effect of ice cover in the Ross and Weddell Seas, atmospheric causal agent was reversed off over ice caries and the top drag coefficient was two-fold to take into account the top friction.

Large Scale Circulation

The zonal circulation of all three models is henpecked by the ACC over much of the possibility domain, as per the transport stream use in Figure 1a for JRA55IAF, which is symbolic of all three models. Semitropical gyres are present in the Atlantic and Indian basins, with the Brazil and Agulhas Currents interacting with the ACC north of the Falkland Ground and south of Cape Agulhas, severally.

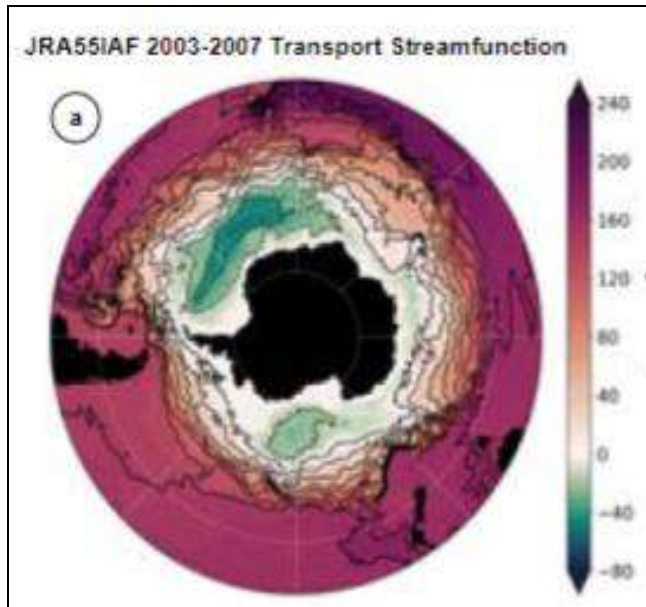


Fig 3: Large Scale Circulation

In this computer memory unit of the model, the northern boundary is at 29.04°S , which is same closeto the latitude of Sugarloaf Point, where the EAC leaves the coast of Australia and flows towards New Sjaelland. As such, the model domain is omit most of its formation region and the result is a very weak current. In these broadstrokes, the models are largely very similar. In that location are fluctuation in, e.g., the position and intensity of the Brazil-Malvinas Blend or the strength of the Agulhas Contemporary. The magnitude shipping through Drake Passage, TACC, is a commonly taken metric function of the zonal stream of the Southern Ocean. Holocene epoch observational estimates give a transportation of 136.7 ± 6.9 Sv (Meredith *et al.*, 2011), based on analysis of historical hydrographic élément, and 173.3 ± 10.7 Sv (Donohue *et al.*, 2016), 285 which includes the barotropic flow. ue to model spinup, internal unevenness of the ocean and vari-ability in the surface forcing (for JRA55IAF and JRA55ABS), the particular five year period chosen for the average value can lead to occurrent in both the mean and stock deviation of TAC

Result

Septet model runs are represented and compared in this section. Each model235run starts on November 8, 2007 and finishes on December 31, 2008. The 236 output was stored hourly. To allow for possibility spin up, and also focus on the 237 year 2008, the output signal for the last 54 days in 2007 was discarded. We note that a spin up time of 30-40 days, observed mainly by the spin up time of the tidal filter (see Appendix B), should be comfortable for the present study. 240 This was habitual by sensitivity studies using different spin up times. To study the driving origin of the S2signal in the ocean, least squares is used to decompose the time-varying atmospherical forcing and ocean re-243sponse at each grid point into a purely curving component with a period of play of 12 hours and a residual. The first group of runs is susceptible only to gravitational forcing (Run T, 248 Run Tn, Run*Tn). The headfirst group (Run S, Run S') is standard atmosphere unscheduled and tidal nudging is set to zero. RunS'is forced byp'a(t) andτ's(t). The next-to-last group of runs (RunTS, RunTnS) allows for tide-surge and tide-tide interaction in the logical thinking of

TWL, some with and without tidal prod. To assess model performance at each tide gauge we calculate the root 259 mean square error (RMSE) from the difference of time series of observa-260tions and predictions. For cite, we also measured the root mean square 261 (RMS) of sight for the same period for each tide gauge.

References

1. Müller M, Haak H, Jungclaus J, S'undermann J, Thomas M. The effect of ocean tides on a climate model simulation. *Ocean Modelling* 2010, 304-313.
2. Pawlowicz R, Beardsley B, Lentz S. Classical tidal harmonic anal-894ysis including error estimates in MATLAB using TTIDE. *Computers &895Geosciences*. 2002;28:929-937. doi:10.1016/s0098-3004(02)00013-4.
3. RA Heine. Department of Geography, Augustana College, Rock Island, IL 61201, USA
4. Schiller A, Fiedler R. Explicit tidal forcing in an ocean general905circulation model. *Geophysical research letters* 34. 2007.
5. Pinter N. Policy forum: One step forward, two steps back on U.S. floodplains, *Science* 2005;308:207-208.
6. Olsen JR, JR Stedinger, NC Matalas and EZ Stakhiv. Climate variability and flood frequency estimation for the Upper Mississippi and Lower Missouri rivers, *J. Am. Water Res. Assoc* 1999;35:1509-1523.
7. Stammer D, Ray R, Andersen OB, Arbic B, Bosch W *et al.*, Accuracy908assessment of global barotropic ocean tide models. *Reviews of Geophysics*90952. 2014, 243–282. doi:10.1201/b18180-3.91052Journal Pre-proofJournal Pre-proof
8. Thompson KR, Wright DG, Lu Y, Demirov E. A simple method920for reducing seasonal bias and drift in eddy resolving ocean models. *Ocean921Modelling* 2006;13:109–125. doi:10.1016/j.ocemod.2005.11.003
9. Weatherall P, Marks KM, Jakobsson M, Schmitt T, Tani S *et al.* A new digital929bathymetric model of the world's oceans. *Earth and Space Science* 2015;2:930331–345. doi:10.1002/2015ea000107
10. Munich Re Group. *Topics Geo—Natural Catastrophes 2006: Analyses, Assessments, Positions*, Munich Re, Munich, Germany 2007.
11. Ward PJ, H Renssen, JCJH Aerts, RT van Balen and J Vandenberghe. Strong increases in flood frequency and discharge of the River Meuse over the late Holocene, *Hydrol. Earth Syst. Sci* 2008;12:159-175.
12. Remo J, N Pinter, B Ickes and R Heine. New databases reveal 200 years of change on the Mississippi River system, *Eos Trans. AGU*, 89(14), doi:10.1029/2008EO140002.
13. Jemberie AA, N Pinter and JWF Remo. Hydrologic history of the Mississippi and Lower Missouri rivers based upon a refined specific-gage approach, *Hydrol. Processes* 2008;22:4436-4447, doi:10.1002/hyp.7046.
14. Criss RE and EL Shock. Flood enhancement through flood control, *Geology* 2001;29:875–878.
15. Helms M, B Bu'chele, U Merkel and J Ihringer. Statistical analysis of the flood situation and assessment of the impact of diking measures along the Elbe (Labe) river, *J. Hydrol* 2002;267:94-114.
16. Jemberie AA, N Pinter and JWF Remo. Hydrologic history of the Mississippi and Lower Missouri rivers based upon a refined specific-gage approach, *Hydrol. Processes* 2008;22:4436-4447, doi:10.1002/hyp.7046.

17. Wales and Scotland. Meteorological Applications: A journal of forecast-934ing, practical applications, training techniques and modelling 16, 13–22.935doi:10.1002/met.124
18. Williams J, Irazoqui Apecechea M, Saulter A, Horsburgh KJ. 937Radiational tides: their double-counting in storm surge forecasts and con-938tribution to the highest astronomical tide. Ocean Science 14, 1057-1068.